Macroscopic Quantum Coherence and Quasidegeneracy in Antiferromagnets

Gregory Levine and Joseph Howard
Department of Physics, Hofstra University, Hempstead, New York 11550
(Received 20 September 1994)

The semiclassical approach to macroscopic quantum coherence (MQC) neglects the intrinsic zero point motion of a vector order parameter when symmetry is approximately unbroken in the ground state. An exact treatment of MQC is carried out on the two-dimensional anisotropic Heisenberg antiferromagnet to illustrate this effect. For small barriers, the order parameter tunneling rate is seen to exhibit the energy scale of the massive rotator states which form the quantum counterpart of classical long range Néel order. Based on these results, predictions relevant to mesoscale magnets are made.

PACS numbers: 75.60.Jp, 03.65.Bz, 76.20.+q

Macroscopic quantum coherence (MQC) is a phenomenon in which an object exists in a quantum superposition of macroscopically distinct states. In connection with MQC, mesoscopic single domain magnetic clusters have been the subject of a number of recent theoretical and experimental investigations [1–6]. In the semiclassical limit, the constituent spins in such a particle are considered to be rigidly coupled together and in the presence of magnetocrystalline anisotropies, the order parameter may "tunnel" back and forth between different orientations. The central prediction of spin MQC theory is an exponential dependence of the order parameter tunneling rate upon the square root of the anisotropy strength K (which may be thought of as the barrier height) and the number of spins N; for an antiferromagnet with exchange constant J,

$$\Gamma \simeq \omega_0 (2NS\sqrt{K/J})^{1/2} \exp(-2NS\sqrt{K/J}), \qquad (1)$$

where the energy scale $\omega_0 \simeq \sqrt{JK}$ [2]. Although considerable experimental support exists for (1), fitting expressions of this type to experiment leads to the conclusion that K is $O(10 - 100)$ times smaller than expected from nominal material parameters [4]. Even more perplexing is the conclusion, based upon widely accepted arguments, that decoherence due to nuclear spins [7,8] would completely suppress MQC at the scale observed in recent experiments on ferritin by Awschalom.

Because of these and other difficulties in interpreting MQC experiments [9,10], it is important to reexamine the MQC phenomenon from first principles and try to figure out where—if at all—the theory has gone astray. The predictions of MQC theory are based on an instanton expansion of a continuum action such as the nonlinear σ model about a spatially uniform saddle point. Like the ferromagnet, the $d \geq 2$ nonlinear σ model has broken symmetry in the ground state, even in a finite geometry. In contrast, the ground state of the Heisenberg antiferromagnet Hamiltonian (HAFM) has long range order without broken symmetry [11,12], and the order parameter possesses low energy dynamics which are independent of a sufficiently small imposed barrier. MQC of a vector order parameter may be understood from such a picture—one in which the order parameter is spatially correlated but strongly *orientationally* delocalized. Thus the starting point of the present study is a finite cluster spin $S = 1/2$ HAFM with an appropriate magnetocrystalline anisotropy term. These are the first exact quantum many body calculations of an MQC effect and are also important in that they address the suitability of instanton calculations in many body Hamiltonians, questioned by Leggett [13] and others.

We have performed exact diagonalizations of the HAFM on two-dimensional square and tilted lattice clusters. We find expression (1) is satisfied for large instanton action, $S_I = 2NS\sqrt{K/J} > S_c$ ($\sim$12). However, for small barriers ($S_I < S_c$)—although no simple analytic expression exists—we find that the tunneling rate is well described by the approximate expression

$$\Gamma \sim \omega_{\rm rot} \exp(-\alpha^2 N^2 S^2 K/J), \qquad (2)$$

where $\omega_{\rm rot} = \beta J/N$ is the energy scale of the quasidegenerate joint states (QDJS) [11,14] that form the quantum counterpart of long range Néel order. In contrast, semiclassical tunneling rates reflect the spin gap energy scale $\omega_0 \sim \sqrt{JK}$. Finite size scaling is used to numerically determine the universal function $\Gamma(J/N, S_I)$ that spans large and small barrier behavior. Most importantly, the delocalized picture leads to much milder conclusions about the effects of coupling to environmental spins than the semiclassical theory of MQC.

We have chosen the anisotropic spin-1/2 HAFM in two dimensions because it is perhaps the simplest model containing the necessary ingredients for MQC:

$$H = J \sum_{\langle \mathbf{i},\mathbf{j} \rangle} \mathbf{S_i} \cdot \mathbf{S_j} - \frac{K}{N} \left(\sum_{\mathbf{i}} (-1)^{\mathbf{i}} S^z_{\mathbf{i}} \right)^2 . \qquad (3)$$

Strong numerical evidence exists to support long range order of the staggered magnetization $\phi_j = (-1)^j S^z_j$ in the pure 2D HAFM ($K = 0$) at zero temperature [12]. The quantity of interest for MQC is the staggered order parameter $\Phi \equiv \sum_j \phi_j$. In the expression above, the 2D

 0031-9007/95/75(22)/4142(4)$06.00

HAFM is modified by a uniaxial anisotropic term to bring about the tunneling of Φ between the configurations $\Phi = \pm\Phi_0$ [15].

According to the theory of MQC, the real time dynamical correlation function $c(t) = \langle 0|\Phi(t)\Phi(0)|0\rangle$, where $\Phi(t)$ is the usual Heisenberg operator, exhibits an oscillation $c(t) = c_0 \sin 2\pi\Gamma t$ at the tunneling frequency Γ. The fluctuation dissipation theorem relates the Fourier transform $c(\omega)$ to the dynamical susceptibility $\chi(\omega)$—the experimentally relevant quantity. For a lattice calculation, standard techniques based on the Lanczos algorithm are available to calculate the complex frequency propagator

$$G_\Phi(z) \equiv \langle 0|\Phi \frac{1}{(z - H + E_0)} \Phi|0\rangle,$$

from which the dynamical correlation function is obtained by an analytic continuation: $-\pi c(\omega) = G''_\Phi(\omega + i\delta)$.

The Lanczos algorithm was used to diagonalize the Hamiltonian (3) and obtain the ground and first excited state energies and many body wave functions on 8, 10, 16, and 18 site lattices with periodic boundary conditions. All energy differences were obtained to a high precision $\Delta E/E \sim O(10^{-13})$. The values of K/J were varied over a range to study the crossover from the extreme quantum limit to the semiclassical limit, $K \sim 0$–1.0 in most cases. Figure 1 shows the results of two typical calculations of $c(\omega)$. The low frequency resonance at Γ results from the coupling of the ground state $|0\rangle$ to the first excited state $|1\rangle$ through Φ. Even though total spin is not a good quantum number once K is nonzero, states $|0\rangle$ and $|1\rangle$ may be thought of as the perturbed singlet and triplet levels, where $|0\rangle$ and $|1\rangle$ differ in the symmetry of the admixture of the two Néel amplitudes. [For lattices of size $N = 4k$ ($N = 4k + 2$), $|0\rangle$ ($|1\rangle$) is the symmetric admixture and $|1\rangle$ ($|0\rangle$) is the antisymmetric admixture with respect to sublattice exchange.] It is seen that with increasing K, Γ shifts to lower frequency as expected.

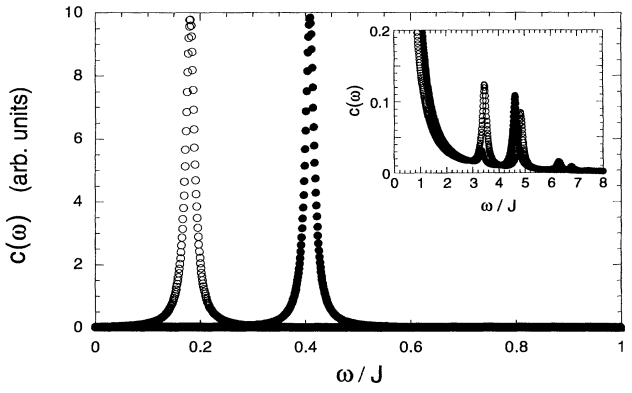

FIG. 1. The dynamical correlation function $c(\omega)$ of the 16-site HAFM for two anisotropies, $K = 0.16$ (solid circles) and $K = 0.48$ (open circles) showing resonances at $\Gamma = 0.409$ and 0.181, respectively. Broadening has been set by $\delta = 0.01$. Inset: full scale plot of spectrum showing higher order resonances ($\delta = 0.001$). The largest secondary peaks have about $1/100$ the spectral weight of the primary peak.

Figure 2 shows the behavior of the tunneling rate Γ with varying lattice size and anisotropy K. A quasilinear regime extending from $K = 0$ is seen, indicating an exponential dependence of Γ upon K over about two decades in Γ/J. We denote this regime the *delocalized* regime (as opposed to the *semiclassical* regime corresponding to large S_I). To obtain the dimensionless constants α and β, finite size scaling is employed. The prefactor of the exponential $\omega_{\rm rot}$ is obtained by looking at the N dependence of Γ at $K = 0$. This is simply the energy gap $E_1 - E_0$ in the absence of anisotropy, and it is shown plotted versus $1/N$ in the inset of Fig. 3. The prefactor $\omega_{\rm rot} \simeq \beta J/N$ with $\beta = 7.6$. As explained later, this expression reflects the energy scale of the QDJS. To determine α, we have computed the slopes of the $\ln(\Gamma/J) \propto K$ data at the $K = 0$ intercept. These slopes are plotted in Fig. 3. It is seen that the slope is proportional to N^2 in agreement with Eq. (2), and we obtain the approximate result for small S_I: $\Gamma \simeq \beta J/N \exp(-\alpha^2 N^2 S^2 K/J)$, where $\alpha \simeq 0.2$.

When the instanton action $S_I = 2NS\sqrt{K/J}$ exceeds $S_c \simeq 12$, the behavior of the tunneling rate crosses over to the semiclassical regime governed by expression (1). Calculations have been carried out to $S_I \sim 26$ to illustrate this crossover. Figure 2 shows an upturn in $\ln\Gamma$ for $K/J > 1.5$. Figure 4 shows the same data plotted as a function of the instanton action, S_I in an N-independent way (explained below). The linear regime, for large S_I, confirms the semiclassical expression (1) rather well [16].

To gain insight into the small barrier limit it is useful to consider how symmetry breaking occurs in an antiferromagnet. The ground state of the HAFM is a singlet $S = 0$, and, therefore, any vector observable including the order parameter Φ must vanish. The order parameter is spatially correlated over the cluster but orientationally delocalized. The symmetry is ultimately broken because a set of NS eigenstates of $\mathbf{S}$ become quasidegenerate for large N; a small perturbation may

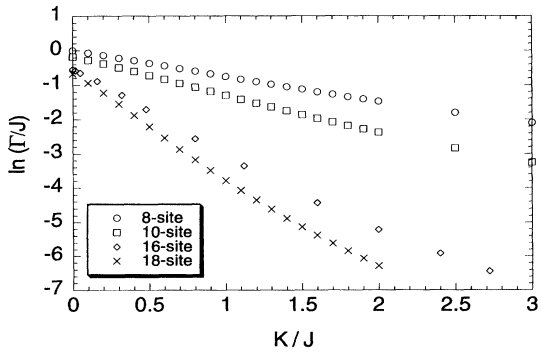

FIG. 2. Logarithm of the tunneling rate Γ showing exponential behavior in K within the *delocalized* regime of small instanton action ($S_I < S_c \sim 12$).

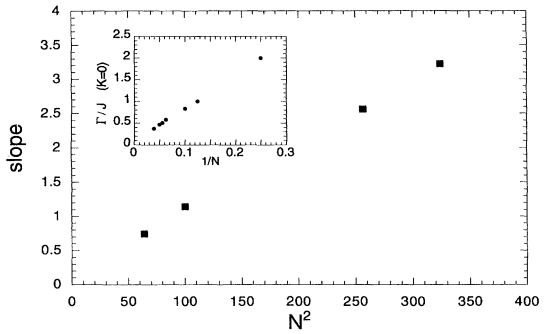

FIG. 3. Finite size scaling of the exponent of expression (2) obtained from the slopes of linear fits to the data of Fig. 2. The tunneling rate is seen to scale as $\exp(-cN^2)$ rather than $\exp(-cN)$ as predicted by the WKB approximation. Inset: Sublattice rotation rate in the absence of anisotropy demonstrating that the energy scale of the QDJS is proportional to N^{-1}. (Points at $N = 20$ and $N = 26$ of inset are from Ref. [12], remaining points are from present work.)

lift this degeneracy resulting in an admixture of states that localize Φ within a solid angle of size $O(1/N)$ [11]. These states, the QDJS, are correspondent with the states of a massive rotator, whose moment of inertia is proportional to N/J [11]. The energy gap $\Delta E = E_1 - E_0$ between the $S = 0$ and $S = 1$ levels is therefore proportional to J/N, in agreement with the finite size scaling demonstrated in Fig. 3.

Recalling that the primary resonance occurs at an energy ΔE, we now consider how ΔE evolves as K is increased from zero. Treating the anisotropy term of (3) as a perturbation yields

$$\Delta E' = J/N - (K/N)[\langle 1|\Phi^2|1\rangle - \langle 0|\Phi^2|0\rangle] \quad (4)$$

to first order. Because the 2D HAFM exhibits long range order at zero temperature, $\lim_{N\to\infty}\langle p|\Phi^2|p\rangle/(NS)^2$ is a constant independent of N and S, where $|p\rangle$ is

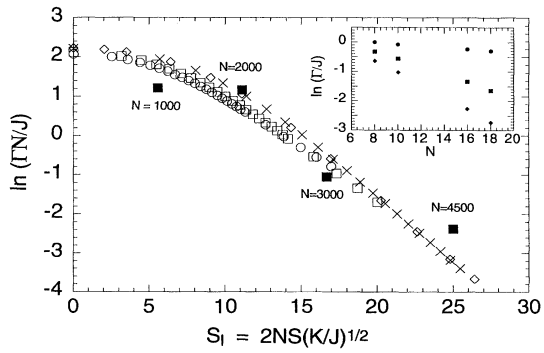

FIG. 4. Scaled tunneling rate versus the instanton action S_I showing universal trend (same symbols as Fig. 2). The crossover to semiclassical behavior appears to occur at $S_I \simeq 12$. Experimental data from Ref. [6] labeled by cluster size N. Shown in the inset are the finite size dependences for three different anisotropies: $K = 0, 1, 2$.

$|0\rangle$ or $|1\rangle$. Defining such a constant $\alpha^2 \equiv [\langle 1|\Phi^2|1\rangle - \langle 0|\Phi^2|0\rangle]/\beta N^2 S^2$ we then obtain

$$\Delta E' = (\beta J/N)[1 - \alpha^2 N^2 S^2 K/J]. \quad (5)$$

Expanding (2) to first order in K, it is seen to agree with (5). Although Eq. (2) is a good approximation in the intermediate S_I region, we can connect the two extremal results, Eq. (1) and Eq. (5), using finite size scaling. From Eq. (5) it is seen that the small barrier behavior of Fig. 4 must be described by a universal (dimension dependent) function of S_I. Rewriting the semiclassical expression (1) $\Gamma \simeq (J/N)S_I^{3/2}\exp(-S_I)$, it is also seen that the large barrier behavior of Fig. 4 must be a universal function of S_I. As shown in Fig. 4, the succession of lattice sizes appears to converge as expected, resulting in a curve that depends only upon the instanton action S_I and *not* upon N explicitly. By comparison to 1D spin chains with integer spin, we conclude that this curve depends only weakly upon the spatial dimension [17]. The self-consistency of perturbation theory leads to the condition $\beta KN\alpha^2 S^2 < \beta J/N$, and, therefore, $S_c^2 = 1/\alpha^2 \sim 25$ provides an estimate of the transition point between delocalized and semiclassical behaviors.

We now turn to experimental signatures of MQC. Garg [7] and Prokof'ev and Stamp [8] have introduced arguments (but based upon semiclassical notions) showing that the prospects for MQC in single domain magnets are extraordinarily unlikely. In the dominant mechanism of nuclear spin decoherence, the local hyperfine coupling of the moments, $H_{\rm hf} = -A\sum \mathbf{I_j}\cdot\mathbf{S_j}$, introduces a fluctuating bias in the double well potential for the tunneling spins and causes strong decoherence.

In the delocalized limit, a very different conclusion is reached. We treat $H_{\rm hf}$ as a perturbation and calculate its effect on each degenerate set of the combined QDJS and nuclear spin systems. This procedure is justified as long as the energy shifts are smaller than Γ. The low energy spectrum of the unperturbed system is described by a degenerate set of states $|p\rangle|\{I_j\}\rangle$, where $p = 0, 1$ refers to the ground and first excited states of the electronic system (the perturbed singlet and triplet levels) and $\{I_j\}$ is the set of possible nuclear spin configurations. The degenerate ground state, $|0\rangle|\{I_j\}\rangle$, has $S_z = 0$, and noting that Φ only couples states with $\Delta S_z = 0$, it is only necessary to consider the $S_z = 0$ elements of the first excited state manifold. In this case, it is possible to show that the first order corrections vanish, $\langle\{I_j\}|\langle p|H_{\rm hf}|p\rangle|\{I_j\}\rangle = 0$, due to the symmetry of the electron spin wave function under sublattice interchange. The second order corrections involve an intermediate state of energy $O(J)$ in which a spin flip has been exchanged between the nuclear and electronic systems. In ferritin, taking $A \sim 50$ MHz and $J \sim 6 \times 10^{10}$ Hz (determined below), the resulting shift in Γ is $O(A^2/J) \sim 4 \times 10^4$ Hz. Thus the spectral weight concentrated in the unperturbed single resonance

is distributed in a multiplet with a width of about 40 kHz; MQC should be observable down to the 1 MHz range. Although particles of this size are semiclassical, exact diagonalizations of HAFMs coupled to nuclear spin degrees of freedom show that the perturbative treatment of nuclear spins works well even for clusters in the semiclassical regime ($S_I \sim 10$). In fact, our results are in disagreement with the conclusions of Refs. [7,8], regarding coupling to environmental spins in the semiclassical regime. Presumably much stronger anisotropy is needed to bring about the conditions consistent with their treatment.

A quantity of considerable experimental interest is the quantum crossover temperature. According to the semiclassical theory of MQC, a resonance peak should emerge below a temperature $T^* \sim \sqrt{JK}$, the temperature at which thermal activation over the barrier has a comparable rate to quantum tunneling. When $S_I \sim S_c$, the order parameter is delocalized and this definition of the crossover does not hold. We have examined the temperature dependent dynamical susceptibility $\chi''(\omega, T)$ on the 10-site lattice for three anisotropies, $K = 0, J, 2J$, and a range of temperatures. In Fig. 5(a), the peak at $\omega \sim 0.1$ (easily seen for $T = 1.0, 1.4$) is the MQC resonance for $K = 2J$. When K is reduced [Fig. 5(b)], the onset temperature of the resonance appears unchanged, rather than reduced. In the small barrier limit, the level spacing dictates T^* and therefore, in experiments in which the particle size is varied, we predict $T^* \propto 1/N$ for particles in the delocalized limit. MQC predicts that T^* has no N dependence.

In the Awschalom experiments on ferritin particles, resonances attributed to MQC for the four particle sizes studied were observed at $\Gamma_{1000} = 1.6 \times 10^8$ Hz, $\Gamma_{2000} = 7.8 \times 10^7$ Hz, $\Gamma_{3000} = 5.6 \times 10^6$ Hz, and $\Gamma_{4500} = 9.5 \times 10^5$ Hz, where the subscript N_{exp} refers to the number of spin-5/2 Fe atoms in the particle. The experimental widths are ~50 kHz, consistent with our estimate. From these data, K and J may be determined by comparison to the universal curve approximated by finite size scaling. $\ln \Gamma N$ is plotted versus N in Fig. 4. The experimental anisotropy ratio, conventionally defined to be $2KS^2/J$, is estimated from the horizontal scale factor in Fig. 4 to be $\sim 1.5 \times 10^{-5}$. A value of the exchange constant $J \sim 6 \times 10^{10}$ Hz is obtained from the vertical scale factor. This anisotropy ratio is larger and somewhat more realistic than a previous estimate of 2.7×10^{-6} in Ref. [4]. In future experiments on smaller clusters it will be interesting to see if the tunneling rate follows the small N behavior anticipated by Fig. 4.

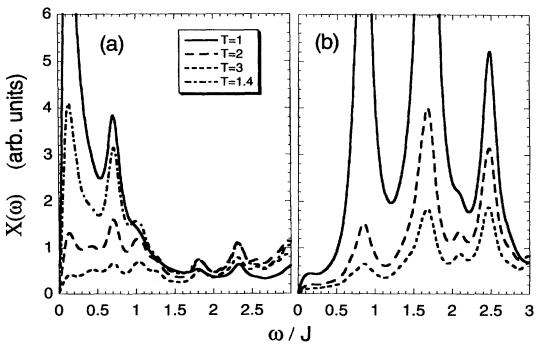

FIG. 5. Finite temperature dynamical susceptibility $\chi(\omega)$ of the 10-site lattice shown for two anisotropies $K = 2J$ (a) and $K = 0$ (b). Resonances are artificially broadened.

G. L. wishes to thank the Aspen Center for Physics for its hospitality and financial support. Research was supported by the Research Corporation and the Pittsburgh Supercomputing Center. J. H. was supported, in part, by the Hauser Scholarship. The authors would like to thank Professor E. M. Chudnovsky, Professor B. F. Friedman, J. H. Miller, Jr., Professor T. O'Dwyer, and Professor W. P. Su.

[1] E. M. Chudnovsky and L. Gunther, Phys. Rev. Lett. **60**, 661 (1988).
[2] B. Barbara and E. M. Chudnovsky, Phys. Lett. A **145**, 205 (1990); I. V. Krive and O. B. Zaslavskii, J. Phys. Condens. Matter **2**, 9457 (1990).
[3] D. D. Awschalom, M. A. McCord, and G. Grinstein, Phys. Rev. Lett. **65**, 783 (1990).
[4] D. D. Awschalom, J. F. Smyth, G. Grinstein, D. P. DiVincenzo, and D. Loss, Phys. Rev. Lett. **68**, 3092 (1992).
[5] D. D. Awschalom, D. P. DiVincenzo, and J. F. Smyth, Science **258**, 414 (1992).
[6] S. Gider, D. D. Awschalom, T. Douglas, S. Mann, and M. Chaparala, Science **268**, 77 (1995).
[7] A. Garg, Phys. Rev. Lett. **74**, 1458 (1995).
[8] N. V. Prokof'ev and P. C. E. Stamp, J. Phys. Condens. Matter **5**, 1663 (1993).
[9] A. Garg, Phys. Rev. Lett. **71**, 4249 (1993).
[10] E. M. Chudnovsky, Phys. Rev. Lett. **72**, 1134 (1994); D. D. Awschalom, D. P. DiVincenzo, G. Grinstein, and D. Loss, Phys. Rev. Lett. **71**, 4276 (1993).
[11] P. W. Anderson, Phys. Rev. **86**, 694 (1952); P. W. Anderson, *Basic Notions of Condensed Matter Physics* (Addison-Wesley, Menlo Park, CA, 1983).
[12] S. Tang and J. E. Hirsch, Phys. Rev. B **39**, 4548 (1989).
[13] See, for instance, A. J. Leggett, in *Chance and Matter,* edited by J. Soultie, J. Vannimenus, and R. Stora (North-Holland, Amsterdam, 1987).
[14] B. Bernu, C. Lhuillier, and L. Pierre, Phys. Rev. Lett. **69**, 2590 (1992).
[15] For $S = 1/2$ the global anisotropy in (3) is the only possible anisotropy.
[16] It is clear from the slope, however, that S_I is approximately 3 times bigger than the true semiclassical action for the system under consideration. We do not understand this apparent discrepancy in the transcription of parameters from the HAFM to the continuum nonlinear σ model.
[17] Comparisons were made to 8- and 10-site $S = 1$ chains. These chains are significantly shorter than their correlation length, making a comparison feasible.